Fast Product Formation and Slow Product Release Are Important Features in a Hysteretic Reaction Mechanism of Glutathione Transferase T2-2†

Per Jemth and Bengt Mannervik*

Department of Biochemistry, Uppsala University, Biomedical Center, Box 576, S-751 23 Uppsala, Sweden

Received December 30, 1998; Revised Manuscript Received April 1, 1999

ABSTRACT: The reaction mechanism of rat glutathione transferase T2-2 has been studied using pre-steady-state and steady-state kinetics. Several parts of the catalytic cycle including binding of substrates, product formation, and product release were investigated. Under saturating conditions, a two-step product release was found to be rate limiting in the enzyme-catalyzed reactions between the nucleophilic substrate glutathione and either of the two electrophilic substrates 1-menaphthyl sulfate and 4-nitrobenzyl chloride. The rate constant for pre-steady-state product formation on rat glutathione transferase T2-2 has an observed pK_a value of 5.7 apparently due to ionization of the sulfhydryl group of glutathione. This rate constant is approximately 2 orders of magnitude higher than k_{cat} at pH values of >6. It can be predicted from the pH dependence that product formation would be the sole rate-limiting step at pH values of <3. A hysteretic mechanism of rGST T2-2 is proposed based on a slow conformational transition detected in pre-steady-state displacement experiments.

Glutathione transferases (GSTs,[1] EC 2.5.1.18) are enzymes that participate in cellular detoxication of endogenous as well as foreign electrophilic compounds. By catalyzing conjugation of the ubiquitous tripeptide glutathione (γ-Glu-Cys-Gly; GSH) with different electrophilic species, GSTs serve the function of facilitating transport of potentially harmful substances out of the cell. Soluble mammalian GSTs can be divided into the seven classes alpha, kappa, mu, pi, sigma, theta, and zeta based on sequence similarity (*1*−*5*); for recent reviews, see Hayes and Pulford (*6*) and Mannervik and Widersten (*7*). After the classification of theta GSTs (*2*, *8*), the function of these enzymes have been revealed in part, but still their catalytic mechanism is not completely elucidated. Class theta GSTs differ from classes alpha, mu, and pi GSTs in that they do not contain a Tyr residue in the N-terminal region used to promote the nucleophilicity of the sulfur group of GSH, but instead contain a Ser residue that may serve this function. This is a feature that class theta GSTs share with GST from *Lucilia cuprina* and GSTs from plants, as shown by site-directed mutagenesis of the *Lucilia* GST and human GST T2-2 (*9*, *10*), and three-dimensional structure determinations of hGST T2-2 (*11*), the *Lucilia* GST (*12*) and a GST from *Arabidopsis thaliana* (*13*). For a recent review of the reaction mechanisms of GSTs, see Armstrong (*14*). Theta class GSTs are believed to be most similar to the ancestral GST from which the alpha, mu, and pi classes evolved (*15*). Thus, from an evolutionary point of view, knowledge about the structure and reaction mechanism of theta class GSTs would be valuable for an understanding of the development and mechanism of action of the younger structures of alpha, mu, and pi GSTs.

In 1973, Gillham performed a kinetic study on a GST purified from rat liver (*16*). The enzyme was catalyzing the conjugation reaction between GSH and aralkyl sulfate esters (*17*). Nearly two decades later, the enzyme was "rediscovered" and grouped into the separate theta class of GSTs (*2*, *8*, *18*). According to the current nomenclature for GSTs (*19*), the enzyme is now called rGST T2-2. Gillham studied the steady-state reaction between 1-menaphthyl sulfate (MS) and GSH catalyzed by rGST T2-2 and proposed that it was best described by an ordered bi-bi mechanism where GSH binds first followed by MS (*16*). Further, the sulfate group, displaced from MS by the attacking thiolate of GSH, was found to leave before the menaphthylglutathione (MSG) adduct. Discrepancies between the kinetic constants obtained by Gillham (*16*) and those from a study on recombinant rGST T2-2 (*20*) led us to undertake a more detailed study of the kinetic mechanism of recombinant rGST T2-2.

This paper presents an investigation of the mechanisms of two reactions catalyzed by rGST T2-2 using a combination of rapid-reaction and steady-state kinetics; the reaction with the classical substrate MS and the reaction with 4-nitrobenzyl chloride (NBC) (Figure 1).

EXPERIMENTAL PROCEDURES

Reagents. MSG was synthesized essentially as described by Hyde and Young (*21*). MS was a kind gift from Dr. B. Gillham, synthesized as described by Clapp and Young (*22*). Other chemicals used were of highest purity commercially available.

† This work was supported by the Swedish Natural Science Research Council and the Swedish Cancer Society.

* To whom correspondence should be addressed. Phone: +46-18-471 45 39. Fax: +46-18-55 84 31. E-mail: Bengt.Mannervik@biokem.uu.se.

[1] Abbreviations: CDNB, 1-chloro-2,4-dinitrobenzene; GSH, glutathione; GST, glutathione transferase; LIST, ligand-induced slow transition; MS, menaphthyl sulfate; MSG, *S*-(1-menaphthyl)glutathione; NBC, 4-nitrobenzyl chloride; NBSG; *S*-(4-nitrobenzyl)glutathione; rGST T2-2, rat glutathione transferase T2-2.

10.1021/bi983065b CCC: $18.00
Published on Web 07/13/1999

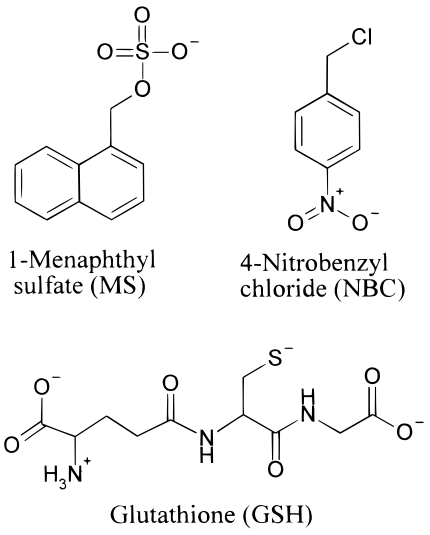

FIGURE 1: Structures of the substrates used in the study of rGST T2-2: 1-menaphthyl sulfate (MS), 4-nitrobenzyl chloride (NBC), and the reactive thiolate form of glutathione (GSH).

Protein Expression and Purification. Recombinant rGST T2-2 was expressed in *Escherichia coli* strain XL1-Blue (Stratagene, La Jolla, CA) and purified by a two-step procedure using DEAE-Sepharose-6B and affinity chromatography using ferric ions immobilized on an IDA-Sepharose column (Pharmacia Biotech, Uppsala, Sweden) as described elsewhere (*20*).

Steady-State Kinetics. If not otherwise stated, reactions were carried out at 15 °C in 0.1 M sodium acetate (pH 4.0−5.6), 0.1 M sodium phosphate (pH 5.9−8.1), or 0.1 M sodium glycine (pH 9.0−11.0). The activities toward NBC and 1-chloro-2,4-dinitrobenzene (CDNB) were measured as described by Habig et al. (*23*) and the activity with MS as described by Gillham (*17*). For determination of kinetic constants, the activity was measured at different concentrations of the variable substrate, and several replicates were made at each concentration. For determinations of k_{cat}^{NBC}, the GSH concentration was held constant at 10 mM and the concentration of NBC was varied between 4 and 200 μM. All k_{cat} values were calculated per subunit (27.3 kDa). Owing to the low K_M^{MS} value of rGST T2-2 [1 μM (*20*)], k_{cat} in the MS reaction was determined at constant MS (25 μM) and varying GSH concentration (0.30−20 mM). For determination of the K_I value for *S*-(4-nitrobenzyl)glutathione (NBSG), a ThermoMax microplate reader (Molecular Devices, Menlo Park, CA) was used to measure the enzyme-catalyzed conjugation of CDNB and GSH in 0.1 M sodium phosphate, pH 6.0, at 30 °C, in the presence of varying concentrations of NBSG. Eight CDNB concentrations (0.030−1.0 mM), three GSH concentrations (0.1, 1, 10 mM), and five inhibitor concentrations (0−100 μM) were used and duplicates were measured for each concentration. Using nonlinear regression analysis, the equation

$$v = [V[\mathrm{CDNB}][\mathrm{GSH}]]/[K_M^{CDNB}K_M^{GSH}(1 + [I]/K_I) + K_M^{GSH}[\mathrm{CDNB}] + K_M^{CDNB}[\mathrm{GSH}] + [\mathrm{CDNB}][\mathrm{GSH}]] \quad (1)$$

was fitted to experimental data by the program SIMFIT (*24*). K_I^{MSG} and $K_I^{sulfate}$ were determined in 0.1 M sodium phosphate, pH 7.5, at 15 °C, by measuring activity at different concentrations of GSH (0.5−20 mM, 3−5 concentrations per MS concentration), MS (2−50 μM, 4 concentrations per inhibitor concentration), MSG (0, 0.5, 5, and 11 μM), and sodium sulfate (0, 0.50, 1.0, and 2.0 mM). At least three determinations of the reaction rate were made at each combination of substrates and inhibitor. K_I^{MSG} was calculated by fitting

$$v = [V[\mathrm{MS}][\mathrm{GSH}]]/[K_M^{MS}K_M^{GSH}(1 + [I]/K_I) + K_M^{GSH}[\mathrm{MS}](1 + [I]/K_I) + K_M^{MS}[\mathrm{GSH}] + [\mathrm{MS}][\mathrm{GSH}]] \quad (2)$$

to experimental data, and $K_I^{sulfate}$ was calculated by fitting the equation

$$v = [V[\mathrm{MS}][\mathrm{GSH}]]/[(1 + [I]/K_I)(K_M^{MS}K_M^{GSH} + K_M^{GSH}[\mathrm{MS}] + K_M^{MS}[\mathrm{GSH}] + [\mathrm{MS}][\mathrm{GSH}])] \quad (3)$$

to data. The equations were written as user-supplied models for the qn-fit program of the SIMFIT package (*24*). Equations 1−3 are simplified models for a rapid-equilibrium random mechanism in which possible interactions in the binding of the reactants are neglected (*25*); eq 1 competitive inhibition with both substrates; eq 2 competitive with GSH, noncompetitive with MS; eq 3 noncompetitive with both substrates (*25*). Model discrimination was based on the results of the regression analysis and involved graphs, residuals, and statistical criteria (*24*, *26*). Steady-state activity was also measured at constant concentrations of MS (25 μM, saturating) and GSH (0.50 mM, not saturating) and at varying concentration of MSG (0−120 μM) in 0.1 M sodium phosphate, pH 7.5, at 30 °C. Activity in the presence of sucrose was measured at 30 °C in 0.1 M sodium phosphate, pH 7.5, and saturating concentrations of GSH and MS (10 mM and 25 μM, respectively). Values for the relative viscosities used (1.00, 1.22, 1.47, 2.48, and 3.15) were estimated using the values given by Brouwer and Kirsch (*27*).

Stopped-Flow Measurements. Pre-steady-state kinetics of rGST T2-2 were investigated using a stopped-flow spectrophotometer from Applied Photophysics (Leatherhead, Kent, U.K.). Experiments were performed mainly at 15 °C in the buffers used for steady-state kinetics. Equal volumes of the reactants were mixed in the experiments, and final concentrations (of e.g. enzyme, substrates or ligands) in the measuring cell are given. For definition of rate constants, see reaction schemes and Figure 2.

Activities with MS and NBC were measured by mixing enzyme−GSH complex with the electrophiles and monitoring formation of product as described in the references cited above for steady-state kinetics. The concentration of rGST T2-2 in these experiments varied between 3 and 10 μM subunit and the GSH concentration was held constant at 10 mM. The concentrations of the different electrophiles were varied as follows: MS, 10−200 μM, and NBC, 2.5−200 μM. Activity measurements with constant MS concentration (25 μM) and varying GSH concentration (0.2−30 mM) were also performed. In the pH dependence study of k_4 with MS as second substrate, three determinations of k_{obs} were made at each pH value by mixing enzyme−GSH complex (3 μM rGST T2 subunit, 10 mM GSH, final concentration) with 25 μM MS and 50 mM buffer (final concentration) and

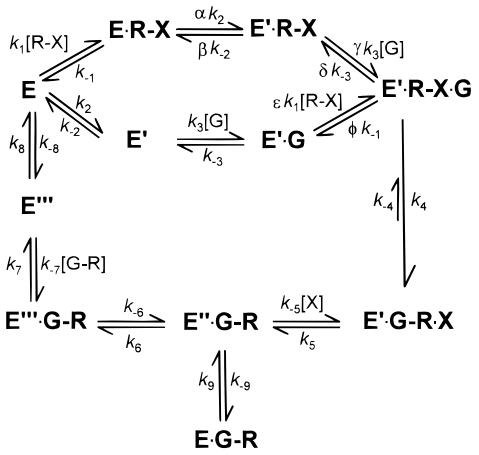

FIGURE 2: Complete reaction scheme for the rGST T2-2-catalyzed reaction, based on the different steps studied.

measuring product formation at 298 nm. At 25 μM MS, k_{obs} is essentially equal to k_4. Each of the three rate determinations consisted of five individual traces run sequentially.

Binding of GSH to rGST T2-2 was measured by mixing GSH with the enzyme and detecting (1) tryptophan fluorescence quenching ($\lambda_{excitation}$ = 290 nm; emission of light at wavelengths > 320 nm was measured using a cutoff filter) and (2) the change in absorbance at 239 nm (*28*). The GSH concentration was varied between 0.15 and 10 mM at a constant subunit concentration of 10 μM. Binding of GSH to rGST T2-2 in the presence of product (10 μM subunit, 20 μM NBSG; or 10 μM subunit, 10 μM or 20 μM MSG) was detected by measuring increase in tryptophan fluorescence similarly as above. Binding of the reaction products MSG and NBSG to rGST T2-2 was measured by tryptophan fluorescence quenching similarly as for GSH using 1−10 μM rGST T2 subunit. Observed rate constants used in the pH study of product binding were determined in a final buffer concentration of 50 mM.

To obtain observed rate constants, k_{obs}, either a single or double exponential equation or a single exponential with steady state was fitted to the data using the software supplied with the apparatus. If the observed rate of ligand binding showed a positive linear concentration dependence (e.g., GSH binding), k_{obs} was plotted against ligand concentration and linear regression analysis was used to obtain values for k_{on} and k_{off} according to

$$k_{obs} = k_{-3} + k_3^{app}[GSH] \quad (4)$$

If k_{obs} showed a negative concentration dependence, which occurred in the displacement experiment with product and GSH, the equation

$$k_{obs} = k_9^{app} + k_{-9}^{app} K'_S/(K'_S + [GSH]) \quad (5)$$

was fitted to the data. K'_S in eq 5 is interpreted as a dissociation constant and is the quotient between the rate constants in a concentration dependent GSH-binding step (k_{-3}/k_3^{app}) after that described by k_9^{app}. When the actual chemical transformation on the enzyme was investigated, the following equations were fitted to experimental data

$$k_{obs} = k_4[S]/(K_{0.5} + [S]) \quad (6)$$

$$k_{obs} = k_{-4} + k_4[S]/(K_{0.5} + [S]) \quad (7)$$

where [S] is the concentration of the substrate varied. In these cases, there are actually two relaxation times involved, but the first one, binding of the second substrate, is described by eq 4 (when GSH is varied) and is spectroscopically silent. $K_{0.5}$ in eqs 6 and 7, the substrate concentration at which $k_{obs} = k_4/2$, equals $(k_{-3} + k_4)/k_3^{app}$ (when GSH is varied) or $(k_{-1} + k_4)/k_1$ (when the electrophile is varied). k_1, k_{-1}, k_{-3}, and k_3 are rate constants for binding of the varied substrate (see reaction schemes in the Results). At high enough concentration of the second substrate, k_{obs} approaches the true rate constant for the catalytic step, k_4. When k_{obs} did not show a concentration dependence, the average of the obtained values was used as a measure of the true rate constant in the reaction studied (owing to the large value of k_1^{MS}, this was the case for k_4 in the reaction with varying MS and saturating GSH concentration). Each k_{obs} obtained was an average of 4−12 different traces run sequentially on the stopped-flow spectrophotometer. The theory of pre-steady-state kinetics is described by Fersht (*29*).

The pH dependence of different kinetic parameters (*29*) was studied at 15 °C. Using the SIMFIT program, a first or second-degree rational function was fitted to obtained rate constants plotted against hydroxide ion concentration.

Microcalorimetry. Isothermal microcalorimetric titrations were performed with a 2277 Thermal Activity Monitor (Thermometric, Järfälla, Sweden) at 30 °C. The calorimeter was dynamically calibrated before each experiment, using electrically generated heat pulses as recommended by the manufacturer. An experiment consisted of 15 or 26 injections of 10 μL of ligand solution, 10 s duration, into a 2 mL stirred titration vessel initially containing 1.000 mL of enzyme solution in the same buffer as the ligand. Buffers used were 0.10 M sodium phosphate at different pH values. The concentration of rGST T2-2 in the vessel was 20−100 μM. Ligand concentrations in the syringe were typically 0.50−5.0 mM. The exact concentration used in an experiment was optimized with regard to the affinity of the enzyme for the ligand under the conditions used. Titration data were corrected for the heat generated by addition of the ligand not due to enzyme−ligand interactions. Data analyses were carried out to estimate the binding parameters using the program Digitam for Windows provided with the instrument.

RESULTS

Enzyme Preparation. rGST T2-2 used in this study was expressed and purified according to the protocol described by Jemth et al. (*20*). The values of the kinetic constants and the specific activity with MS (*20*) differ considerably from those given by Gillham (*16*, *17*). However, since orthologs of GST T2-2 from different species are the only enzymes known to catalyze the reaction between MS and GSH, there should be no doubt that rGST T2-2, used by Jemth et al. (*20*) and in this study is the same enzyme as that previously investigated by Gillham (*16*, *17*).

Initial Rate Studies and Product Inhibition. As a starting point for the investigation of the catalytic mechanism of rGST T2-2, steady-state initial rates were measured by varying the concentrations of MS and GSH in absence and presence of the products MSG and sulfate. The reciprocal

of the initial rate, $1/v$, was plotted against 1/[substrate] in the absence of product. The lines corresponding to fixed concentrations of the second substrate were not parallel but intersected, thus, the reaction mechanism is sequential (results not shown). To check the inhibition pattern of the two products sulfate and MSG, a study similar to that by Gillham (*16*) was performed. Sulfate was found to be clearly noncompetitive with respect to both substrates in the MS reaction [change in both k_{cat} (the turnover number at saturating substrate concentrations) and K_M values]. MSG was found to be close to competitive (change only in K_M value) with respect to GSH, but noncompetitive with respect to MS (results not shown). This is in accordance with previous results (*16*). The secondary plots of $1/k_{cat}$ and K_M/k_{cat} were found to be linear or possibly hyperbolic with inhibitor concentration. Only three inhibitor concentrations were used, in our experiments as well as in Gillham's (*16*), and this is not enough to accurately judge whether linear or hyperbolic behavior is observed. To cover a wider range and to get more experimental points, the MSG concentration was varied (1−120 μM) at constant substrate concentrations and $1/v$ was plotted against MSG concentration. The data could be described by a 2:1 rational function with two asymptotic slopes, one approximating the curve in the range 0−5 μM and one at higher MSG concentrations. This result shows that the above replots of $1/k_{cat}$ and K_M/k_{cat} are indeed nonlinear, contrary to the previous interpretation. This rate behavior indicates that there are more than one enzyme form in the reaction scheme that can bind MSG. Thus, the observed inhibition pattern does not point to an ordered mechanism but rather to a random reaction mechanism. Keeping this in mind eqs 2 and 3, although too simple to describe the experiments completely since they do not take into account the existence of additional enzyme forms, were fitted to the data sets obtained from the inhibition studies. The apparent K_I values were determined as 3.2 ± 0.3 μM and 0.61 ± 0.03 mM for MSG and sulfate, respectively.

Effect of Viscosity on Steady-State Kinetics. Another clue to the reaction mechanism was obtained from activity experiments in the presence of the viscosogenic reagent sucrose. It has been shown that the rate of a diffusion-controlled reaction is dependent on the viscosity in the medium in which the reaction takes place [see Brouwer and Kirsch (*27*) and references therein]. Also, viscosity could affect the catalyzed reaction if it is dependent on fluctuations between conformational substates [cf. Beece et al. (*30*) and references therein]. The activity of rGST T2-2 was measured under saturating conditions with MS and GSH, and it was found that the quotient between enzymatic rate in absence and presence of sucrose is lineary dependent on the relative buffer viscosity with a slope of 0.65 ± 0.05. The fractional viscosity dependence suggests that solvent-dependent conformational transitions are rate contributing. Another viscosogen, glycerol, was used to verify that sucrose did not work as a nonspecific inhibitor of the enzyme [cf. Bazelyansky et al. (*31*)].

To gain further insight into the reaction mechanism of rGST T2-2, pre-steady-state measurements were performed on the different possible steps on the reaction pathway of the enzyme. Rate constants and schemes referred to in the text are compiled in a complete proposed reaction scheme in Figure 2.

Scheme 1

$$E \underset{k_{-1}}{\overset{k_1[R\text{-}X]}{\rightleftharpoons}} E\bullet R\text{–}X$$

$$E\bullet G \underset{\phi k_{-1}}{\overset{\varepsilon k_1[R\text{-}X]}{\rightleftharpoons}} E\bullet R\text{–}X\bullet G$$

In this and following reaction schemes, E is the enzyme subunit, G is GSH or the glutathionyl moiety of GSH, and R−X is the electrophilic substrate. X in the electrophilic substrate is the leaving group in the reaction, i.e., sulfate in MS and chloride in NBC, and R is the methylnaphthyl part of MS or the benzyl group of NBC.

Pre-Steady-State and Equilibrium Binding of the Electrophilic Substrate. The catalyzed reaction starts with binding of the substrates to the active site, one GSH and one molecule of the electrophilic substrate. Each of the two subunits of rGST T2-2 contains four tryptophan residues which makes the enzyme suitable for binding studies utilizing quenching of the intrinsic fluorescence by the ligands. However, binding of the electrophilic substrates MS and NBC could not be monitored directly by time-resolved change in fluorescence. The lack of measurable time-resolved change in fluorescence upon binding of MS or NBC to rGST T2-2 could be due to absence of fluorescence quenching. However, since it was found that the GSH conjugates of the two substrates quench the fluorescence of rGST T2-2 much more than GSH, it is likely that the reason is not absence of quenching but a large value of the on rate for the electrophile (k_1) (Scheme 1). Inner filter effects with NBC and fluorescence of MS also interfered with the intrinsic fluorescence of rGST T2-2, and therefore, it was not possible to tell whether quenching of the fluorescence had occurred. Nevertheless, the rate constant for binding of NBC, when GSH is bound to the enzyme (ϵk_1^{NBC}, Scheme 1), can be estimated from the hyperbolic concentration dependence of the observed rate constant for pre-steady-state burst of product formation (k_4), to be at least 3×10^5 M^{-1} s^{-1} at 15 °C. In a similar fashion, the on rate for MS (ϵk_1^{MS}) can be estimated as $>10^7$ M^{-1} s^{-1}, close to the diffusion limit. These experiments are discussed in further detail under Pre-Steady-State Product Formation.

Equilibrium binding experiments using isothermal titration microcalorimetry showed that the enzyme can bind MS also in the absence of GSH. The binding curves from the microcalorimetric experiments with MS indicate a stoichiometry of approximately 0.8 (results not shown). By taking the mean of the results from several experiments, K_D^{MS} was calculated as approximately 10 μM. Thus, binding of electrophile to free enzyme is possible and the association rate constant appears to be close to the diffusion limit for binding to enzyme−GSH complex, and most probably to free enzyme as well. On the basis of the large value of ϵk_1^{MS} and the K_D^{MS} value, k_{-1} is estimated to be >100 s^{-1} for MS.

Pre-Steady-State Binding of GSH. Binding of the other substrate, GSH, was measurable using the intrinsic fluorescence of rGST T2-2. After rapid mixing, the rate of binding of GSH to rGST T2-2 was monitored as time-resolved quenching of the fluorescence in the stopped-flow spectrofluorometer. The change in fluorescence followed a single-exponential decay, and the observed rates showed a linear dependence on GSH concentration in the concentration range

Table 1: Kinetic Constants[a] at 15 °C, pH 7.5, for the Reactions of GSH with 4-Nitrobenzyl Chloride and 1-Menaphthyl Sulfate, Catalyzed by rGST T2-2

electrophilic substrate	k_3^{app} [b] (10^3 M^{-1} s^{-1})	k_{-3} (s^{-1})	k_4[c] (s^{-1})	k_6 (s^{-1})	k_7 (s^{-1})	k_{-7}^{app} (10^6 M^{-1} s^{-1})
4-nitrobenzyl chloride	1.2 ± 0.1	1.2 ± 0.3	20 ± 3	0.5 ± 0.2	2.7 ± 0.6	0.36 ± 0.02
1-menaphthyl sulfate			37 ± 8	1.9 ± 1.7	8 ± 6	1.6 ± 0.4

electrophilic substrate	k_9^{app} [d] (s^{-1})	k_{-9}^{app} (s^{-1})	K'_S (mM)	k_{cat}[f] (s^{-1})	K_M^{NBC} (μM)	K_M^{GSH} (mM)
4-nitrobenzyl chloride	0.08 ± 0.01	0.40 ± 0.08	1.2 ± 0.5	0.23 ± 0.03	20 ± 12	
1-menaphthyl sulfate	0.23 ± 0.03	19 (PE[e])	PE	0.73 ± 0.03		1.0 ± 0.2

[a] Kinetic constants that are not steady-state parameters are defined by the reaction scheme in Figure 2. [b] k_3^{app}, k_{-3}, and k_6, k_7, and k_{-7}^{app} were calculated by linear regression analysis of observed relaxation rate constants. k_3^{app} and k_{-3} are measured in absence of electrophilic substrate. [c] k_4 is the pre-steady-state rate constant for product formation on rGST T2-2. To obtain k_4 for NBC, eq 6 was fitted to k_{obs} plotted versus GSH concentration. For MS, the value of k_4 was calculated by taking the mean of observed rate constants since $k_{obs} \approx k_4$ in the range of MS concentrations studied. This is due to the high value of the on rate for MS (k_1), but it probably results in a slight underestimation of k_4. [d] The values of the rate constants k_9^{app} and k_{-9}^{app}, and that of K'_S, were obtained by fitting eq 5 to experimental data. [e] PE, poorly estimated, the experimental error is larger than the parameter value. [f] k_{cat} and K_M are steady-state parameters of the catalyzed reaction. They were determined under similar conditions as k_4 except that data were collected after the initial burst phase. k_{cat} and K_M were calculated by fitting the Michaelis−Menten equation to experimental data. For the NBC reaction, the electrophile was varied at saturating GSH concentration and for MS saturating MS concentration and varying GSH concentration was employed. See Experimental Procedures for additional details.

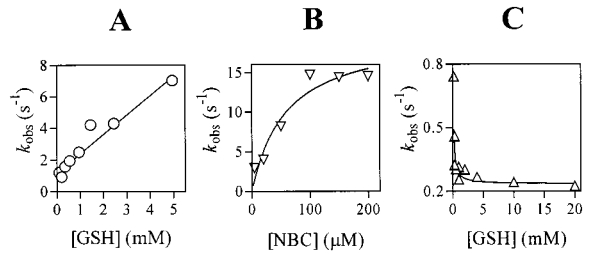

FIGURE 3: Examples of plots used to determine microscopic rate constants at 15 °C, pH 7.5. (A) The observed rate constant for binding of GSH to rGST T2-2 showed linear dependence with GSH concentration. The slope of the curve was interpreted as the on rate (k_3^{app}) and the intercept with the *y*-axis as the off-rate (k_{-3}) of the equilibrium between GSH and rGST T2-2 (eq 4). The values for on and off rates of the reaction products MSG and NBSG were determined in a similar fashion. (B) The pre-steady-state formation of NBSG on the enzyme showed a hyperbolic dependence on the NBC concentration. k_4, the observed rate at infinite NBC concentration, was determined by fitting a first-degree hyperbolic function (eq 6) to experimental data. The slope of the curve at the origin was used to estimate ϵ k_1^{NBC}. (C) Observed rate constants of GSH binding determined by displacement of MSG from rGST T2-2. Equation 5 was fitted to data in order to estimate k_9^{app} and k_{-9}^{app}.

used. Using eq 4, the constants for the apparent on rate (k_3^{app}) and the off rate (k_{-3}) for GSH binding to free enzyme were calculated (Table 1, Figure 3A, Figure 4A). Binding of substrates is often diffusion controlled, i.e., the second-order rate constant for the association should be $>10^7$ M^{-1} s^{-1}. The present results show clearly that binding of GSH to rGST T2-2 is not diffusion controlled given an apparent association rate constant k_3^{app} of 1.2×10^3 M^{-1} s^{-1} at 15 °C, suggesting that more than one step is involved in the binding. Caccuri et al. (*32*) have recently shown that several distinct steps are involved in the binding of GSH to GST P1−1. For rGST T2-2, the low association rate constant for GSH is most probably due to a rapid preequilibrium involving a spectroscopically undetectable conformational transition in the enzyme structure represented by k_2 and k_{-2} in Scheme 2.

If $k_{-2} \gg k_2$, k_3 will appear much lower than its actual value. The off rate constant for GSH (k_{-3}) was determined as 1.2 s^{-1} at 15 °C (Table 1), giving an approximate equilibrium dissociation constant of 1 mM. The experiment shows that binding of GSH to free rGST T2-2 is possible, in accordance with a random mechanism.

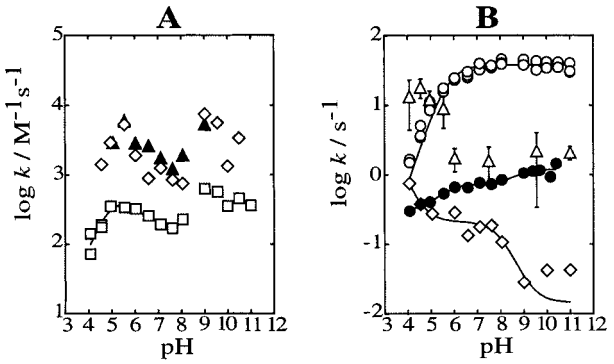

FIGURE 4: pH dependence at 15 °C for different kinetic parameters in the reaction between MS and GSH catalyzed by rGST T2-2. (A) k_3^{app} (▲) was obtained by measuring intrinsic tryptophan fluorescence quenching of rGST T2-2 at different GSH concentrations (0.30−10 mM) as described in the Experimental Procedures. k_{cat}/K_M^{GSH} values (□) were determined by varying the GSH concentration (0.30−20 mM) at constant MS concentration and fitting a first degree rational function to obtained data. $k_4/K_{0.5}^{GSH}$ values (◇) were obtained by fitting a first degree rational function to observed rate constants of the pre-steady-state formation of MSG on the enzyme when the GSH concentration was varied at constant MS concentration (the enzyme was preincubated with MS). (B) k_{cat} values (●) were obtained by varying the GSH concentration (0.3−20 mM) at saturating MS concentration. Values for k_4 (○) were obtained at constant GSH (10 mM) and MS concentration (25 μM). The enzyme was preincubated with GSH. Each value is an average of five different measurements. Rates of product release, $k_6k_7/(k_6 + k_7)$ (△), were obtained by measuring intrinsic tryptophan fluorescence quenching of rGST T2-2 at different MSG concentrations. Values for k_9^{app} (◇) were obtained by measuring displacement of MSG by GSH at different GSH and constant enzyme-MSG concentrations as described in the Experimental Procedures. To obtain apparent pK_a values, either a first or second degree rational function was fitted to data. Apparent pK_a values were determined as 5.5 ± 0.2 and 8.7 (k_{cat}, the basic pK_a value was poorly estimated), 5.7 ± 0.1 (k_4), 1.9 and 8.1 (k_9^{app}), and 4.7 and 5.9 (the two most acidic pK_a values of k_{cat}/K_M^{GSH}).

The binding of GSH was also monitored as increase in absorbance at 239 nm, reflecting formation of the reactive GSH thiolate ion (*28*). The observed rate constants at different GSH concentrations were similar to those obtained using fluorescence quenching, indicating that deprotonation of GSH is fast (data not shown). At high concentration of GSH, the observed rate constants are predicted to show a

Scheme 2

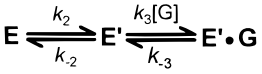

Scheme 3

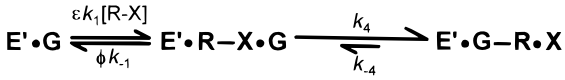

hyperbolic dependence on GSH concentration, when the rate of deprotonation of GSH becomes limiting (*32*).

Pre-Steady-State Product Formation. After binding of both substrates and deprotonation of GSH, the products are formed on the enzyme by nucleophilic attack of the GSH thiolate on the methylene sulfate or methylene chloride group of MS or NBC, respectively. The pre-steady-state formation of products on the enzyme was measured as increase of absorbance at 298 nm for the MS reaction and at 310 nm for the NBC reaction. Clear bursts of product formation were obtained for both reactions, suggesting that at least one subsequent step on the reaction pathway is slower than that for formation of products. The amplitude of the burst was found to correspond to the concentration of active sites present in the experiment. Hence, both active sites in the dimeric rGST T2-2 seem to catalyze the reaction. To obtain observed rate constants, a single exponential equation was fitted to experimental traces. The observed rate constant increased hyperbolically with the NBC concentration at constant GSH concentration (enzyme preincubated with GSH). It also increased hyperbolically with GSH concentration when enzyme was preincubated with MS, but was found to be independent of the MS concentration (10−200 μM) when enzyme was preincubated with GSH. At low enough concentration of MS, k_{obs} is expected to show a hyperbolic dependence, similarly as for NBC and GSH, but presumably owing to a large association rate constant k_1^{MS}, this is not observed experimentally. Instead, the mean of several observed rate constants was calculated to estimate the true rate constant k_4^{MS} (Scheme 3, Table 1). To obtain values of k_4^{NBC} (Figure 3B, Table 1) and of k_4^{GSH} (constant MS, varying GSH), eq 6 was fitted to observed rate constants. The value of k_4^{GSH}, obtained after fitting of eq 6 to experimental data, was found to equal k_4^{MS} (constant GSH preincubated with the enzyme, constant MS) as would be expected. Hence, the choice of experimental approach did not affect the k_4 value obtained. Scheme 3 shows the reaction steps and rate constants involved in the determination of k_4 using enzyme preincubated with GSH.

The pre-steady-state rate constant for product formation on the enzyme k_4 was found to be high compared to the k_{cat} values of rGST T2-2 (Table 1, Figure 4B). With MS as electrophilic substrate, k_4 was found to be approximately 40 s^{-1} at 15 °C, pH 7.5, thus 50 times higher than k_{cat} under those conditions. k_4 with NBC as second substrate was also found to be substantially higher than the corresponding k_{cat}. It should be noted that the rate constant for the reverse reaction, k_{-4}, is numerically redundant in the regression analysis such that eq 7 reduces to eq 6. The constant k_{-4} should be present, but the experimental data at low substrate concentrations are not accurate enough to give reliable parameter values.

As mentioned previously, the observed pre-steady-state rate constant for product formation when MS was preincubated with enzyme and rapidly mixed with GSH showed a hyperbolic dependence with GSH concentration. The reaction steps and rate constants describing this experiment are shown in Scheme 4.

At high GSH concentration, k_{obs} is limited by k_4 (giving the hyperbolic behavior), but at low GSH concentration the observed rate constant should reflect the steps prior to k_4, those involved in GSH binding (αk_2, βk_{-2}, γk_3, δk_{-3}).The slope of the hyperbolic curve at the origin (this slope will be referred to as $k_4/K_{0.5}^{GSH}$) was found to be numerically equal (within the experimental error) to the apparent rate constant for binding of GSH to free enzyme (k_3^{app}) at all pH values tested (Figure 4A). This indicates that binding of GSH to rGST T2-2 is independent of the presence of a bound electrophilic substrate, or in other words, α, β, and γ in Scheme 4 are all close to unity.

pH Dependence of the Rate Constant for Product Formation k_4. The rate constant k_4 (determined with enzyme preincubated with GSH, Scheme 3) for the catalyzed reaction between MS and GSH increases with pH with an apparent pK_a value of 5.7 ± 0.1 (Figure 4B). k_{cat} with MS as second substrate is much lower than the rate constant for formation of product on the enzyme at all pH values studied. It may be predicted from Figure 4B that k_4 will become the sole rate-limiting step at pH values of <3. Unfortunately, rGST T2-2 is unstable already at pH 4.0−4.5, and determinations of k_4 and k_{cat} cannot be made at lower pH values. Nevertheless, the apparent pK_a value for k_{cat} of 5.5 (Figure 4B) suggests that k_4 (pK_a 5.7) actually contributes to k_{cat} at pH <6; however, the slope is much less than 1, indicating contributions from more than one titratable group. The pH dependence of k_4 reflects proton equilibria in the ternary complex enzyme·GSH·MS. The pH dependence of k_{cat}/K_M^{GSH}, $k_4/K_{0.5}^{GSH}$, and k_3^{app} (Figure 4A) should reflect titrations in the enzyme·MS complex and GSH or in free enzyme and GSH. Since the pH dependences of k_{cat}/K_M^{GSH}, $k_4/K_{0.5}^{GSH}$, and k_3^{app} are all different from that of k_4 (Figure 4), the pH dependence of k_4 most probably reflects titration of the thiol group of the enzyme-bound GSH.

Pre-Steady-State and Steady-State Enzyme−Product Association and Dissociation. In the two reactions studied there are two substrates and two products. The leaving group in these nucleophilic substitution reactions is chloride (from NBC) or sulfate (from MS). The binding of these did not give a spectroscopically detectable signal and could not be measured by pre-steady-state kinetics. Although the microscopic rate constants (denoted k_5 and k_{-5}) could not be obtained, the quotient k_5/k_{-5} sulfate was determined as 0.6 mM in the inhibition study (15 °C, pH 7.5).

The binding of the other product, the GSH conjugate, could however be detected by measuring quenching of intrinsic

Scheme 4

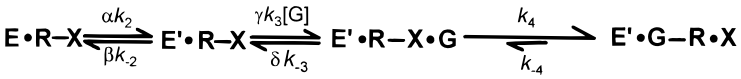

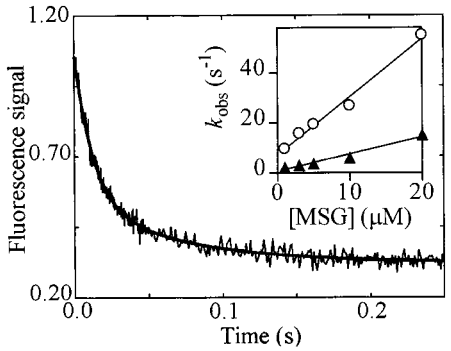

FIGURE 5: Biphasic binding of the reaction product MSG. rGST T2-2 was mixed with MSG, and time-resolved change in fluorescence was monitored. A double exponential equation was fitted to the experimental data points. The two observed rate constants obtained were plotted versus MSG concentration to estimate k_6 (▲, intercept of best-fit curve), k_7, and k_{-7} (○, intercept and slope, respectively, of best-fit curve) using linear regression analysis (inset).

Scheme 5

$$E \underset{k_{-8}}{\overset{k_8}{\rightleftharpoons}} E''' \underset{k_{-7}}{\overset{k_7[G\text{-}R]}{\rightleftharpoons}} E'''\bullet G{-}R \underset{k_{-6}}{\overset{k_6}{\rightleftharpoons}} E''\bullet G{-}R$$

tryptophan fluorescence. The binding of product was judged to be biphasic using SIMFIT (*24*) to analyze the residuals of single and double exponential functions fitted to experimental data. Both observed rate constants seemed to display linear dependence on product concentration, similarly as GSH binding (Figure 5). The equation

$$k_{obs} = k_7 + k_{-7}^{app}[G{-}R] \quad (8)$$

was used to calculate k_7 and k_{-7}^{app} (Table 1). The on rate (k_{-7}^{app}) for both MSG and NBSG was found to be faster than that for GSH but still less than the diffusion limit. Hence, a fast preequilibrium, represented by k_8 and k_{-8}, is probably present on this binding pathway as well (Scheme 5). On the basis of the present experiments, it is not possible to tell whether the second observed rate constant obtained really is lineary dependent on GSH conjugate concentration or not. Since rGST T2-2 is a dimer, it would appear possible that the different subunits bind MSG or NBSG with different affinities. The finding that the amplitudes, corresponding to the two relaxation times in the experiments, are similar (within experimental error) supports this model. The other possible model is shown in Scheme 5.

Here, the second transient is interpreted as a conformational transition in the enzyme−ligand complex, giving a spectroscopically detectable signal. The observed rate constant for such a step should display hyperbolic dependence on ligand concentration with k_{-6} as limiting rate. However, in both models, the observed rate constant would be linearly increasing at low MSG or NBSG concentrations (cf. eq 7), and the off rate k_6 would be the observed rate constant at zero concentration obtained by extrapolation. Therefore, the second transient was also subjected to linear regression analysis to estimate k_6. The value of k_6 [or $k_6k_7/(k_6 + k_7)$ if the subsequent step is taken into account] agrees well with k_{cat} at 15 °C in neutral and basic buffers (Figure 4B, Table 1) and is proposed to be the main rate contributing step under those conditions.

The pre-steady-state burst of product formation on the enzyme disappeared if MSG was added to rGST T2-2 before the rapid mixing of enzyme with substrates (results not shown), further corroborating that product release is rate limiting.

In microcalorimetric experiments, K_D^{NBSG} was determined as 3.5 ± 1.6 μM in good agreement with the value estimated by rapid kinetics (<7.5 μM) and by inhibition experiments (2.3 ± 0.5 μM). Owing to the low values of K_D^{NBSG} and K_D^{MSG}, product inhibition of rGST T2-2 is likely to occur.

Pre-Steady-State Displacement of the Products by GSH. To further investigate the presence of conformational changes suggested by the experiments presented so far, displacement of the reaction products MSG and NBSG with GSH was measured in the stopped-flow spectrofluorometer. MSG and NBSG were found to quench the intrinsic tryptophan fluorescence of rGST T2-2 more than GSH, thus, replacement of either MSG or NBSG with GSH resulted in increase in intrinsic tryptophan fluorescence that could be detected.

When GSH was mixed with either E·MSG or E·NBSG (approximately 6−8 μM subunit−product complex out of a total subunit concentration of 10 μM calculated from the estimated dissociation constants), the increase in fluorescence with time followed that of a single exponential. k_{obs} was found to decrease with increasing GSH concentrations. The inverse concentration dependence of the relaxation time observed is indicative of a slow step followed by a fast step. Equation 5 was then fitted to data in order to estimate k_9^{app}, k_{-9}^{app}, and K'_S (Figure 3C). At least for NBSG, K'_S from eq 5 is close to K_D^{GSH} obtained by dividing k_{-3} with k_3^{app} (Table 1), suggesting that k_9^{app} is associated with a slow step or the sum of several slow steps prior to GSH binding. Similar results were obtained when GSH was replacing MSG, although K'_S was not as well estimated as when NBSG was used. The process of product release followed by GSH binding studied in this experiment no doubt consisted of more steps than those identified in the product and GSH binding experiments since the rate constant k_9^{app} was found to be lower than the dissociation rate constants of both MSG and NBSG from rGST T2-2 (Figure 4B, Table 1). Scheme 6 is a simplification of the pathway describing the experiment. Except for k_9 in Scheme 6, the displacement could proceed via the steps denoted k_6, k_7, k_8, and k_2. Thus, the experimentally determined k_9^{app} and k_{-9}^{app} are not numerically equal to k_9 and k_{-9} in Scheme 6, but they represent a lower limit for the respective rate constant.

Scheme 6

$$E\bullet G{-}R \underset{k_{-9}}{\overset{k_9}{\rightleftharpoons}} E''\bullet G{-}R \overset{\text{several steps}}{\rightleftharpoons} E' \underset{k_{-3}}{\overset{k_3[G]}{\rightleftharpoons}} E'\bullet G$$

At GSH concentrations below K_D^{GSH}, the observed rate increases with GSH concentration and this part is left out in the determination of k_9^{app} and k_{-9}^{app}. This effect, which is not described by eq 5, is probably a result of the fact that the system studied consists of several equilibra and not merely two as accounted for in eq 5. The GSH concentration needs to be higher than K_D^{GSH} to shift the equilibrium between enzyme, product, and GSH toward formation of enzyme−GSH complex, hence, making the dissociation of product

(k_6, k_7, and k_8 in Scheme 5) irreversible. At low GSH concentrations, the equilibrium will be in favor of enzyme−product complex and the requirements for eq 5 to be valid are not satisfied. This makes estimation of k_{-9}^{app} much more ambiguous than that of k_9^{app}, and based on these experiments, it is difficult to judge the distribution between the enzyme forms E•G−R and E″•G−R (Scheme 6).

In Figure 4B, it can be seen that, in contrast to those of k_4 and k_{cat}, the value of k_9^{app} decreases with pH. k_9^{app} decreases as k_{cat} increases at basic pH values ending up 10-fold lower than k_{cat} at pH values of ≥9. A microscopic rate constant on the reaction pathway cannot be lower than the k_{cat} value. Consequently, the catalyzed reaction does not proceed through the step represented by k_9 in Scheme 6. This spectrofluorometrically silent step is proposed not to be on the steady-state reaction pathway but on a pre-steady-state pathway going from an equilibrium enzyme−product complex into the catalytic cycle (Figure 2).

DISCUSSION

To our knowledge, the present investigation is the most detailed study performed on the kinetic mechanism of a theta class GST. By using the stopped-flow technique, several microscopic rate constants on the reaction pathway of reactions catalyzed by rGST T2-2 have been determined, and thereby, new aspects of the catalytic mechanism have been revealed.

According to the results from the pre-steady-state kinetics, rGST T2-2 displays a reaction sequence where the electrophile probably adds to the enzyme before GSH, owing to higher rate of association of electrophile. The rate of GSH binding to free enzyme equals the rate of GSH binding to enzyme−electrophile complex as judged from k_3^{app} and $k_4/K_{0.5}^{GSH}$. However, in vivo the resting enzyme should initially be charged with GSH, owing to its high concentration in the cell (1−10 mM). It is not obvious what physiologically relevant substrates may be, but certain arylalkanes can be metabolically activated to carcinogenic sulfate esters (*8*), similar to MS. If GST T2-2 in the cell is further metabolizing an arylmethyl sulfate, it is likely that the first catalytic cycle proceeds through the pathway with initially bound GSH, but that subsequent cycles start with binding of the electrophilic substrate if its concentration is in the micromolar range or above. Thus, even if the binding of substrates is random in theory, the flux through the pathway with initial binding of electrophile could be much larger in practice.

The actual product formation (k_4) is fast and not rate limiting. Most probably, the pH dependence of the rate constant k_4 for pre-steady-state formation of products reflects titration of the enzyme-bound sulfhydryl group of GSH. This suggests an important catalytic function of rGST T2-2 in increasing the nucleophilicity of GSH by lowering the pK_a of the sulfhydryl group. It is noteworthy that the pK_a value of GSH bound to rGST T2-2 was found to be 5.7, similar to that of GSH bound to another theta class GST, hGST T1−1 (*33*). We believe that this is lower than the pK_as for all other GST-bound GSH described (*32*, *34*−*38*).

No doubt, the leaving-group product sulfate (in the MS reaction) is bound in a defined way to rGST T2-2. The crystal structure of the human ortholog of rGST T2-2, hGST T2-2, reveals a sulfate-binding site that is built up by the four

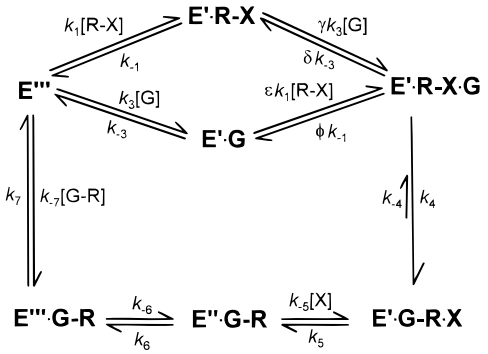

FIGURE 6: Proposed steady-state reaction scheme for rGST T2-2 after adopting the active conformation induced by the reacting substrates.

residues Gln12, Arg107, Trp115, and Arg239 (*11*), all conserved in the amino acid sequence of rGST T2-2. This pocket is probably crucial for the activity with MS. The affinity for sulfate is less than that for the GSH conjugate and therefore sulfate should leave the enzyme first (k_5).

At least two steps in GSH-conjugate product release are slow (k_6, k_7) and determine the steady-state rate under saturating conditions. The structure of human GST T2-2 shows a C-terminal extension as compared to GSTs from other classes, an α-helix that covers the active site. The apo-structure and the GSH and product-liganded structures were all found to be superimposable (*11*). It is likely that the catalytically significant product release steps of rGST T2-2 (k_6, k_7), as well as the fast preequilibria (k_2, k_{-2} and k_8, k_{-8}) and the slow conformational transition (k_9, k_{-9}) are due to motions in the C-terminal extension that has to open up to let ligands in or out. This is probably also the cause of the tight binding of electrophilic substrates and products displayed by rGST T2-2, with low dissociation rates that result from slow helix motions. The significance of catalytically important conformational changes in the tertiary structure of rGST T2-2 is corroborated by the fractional-slope value of the viscosity-dependence of the activity.

The unusual pH dependence of k_{cat}, displaying a slow increase with slopes of <1 from pH 4 until the enzyme is finally denatured at pH values above 11 (Figure 4B), can now be explained by the steps in product release (k_6, k_7) determining the steady-state rate of the enzymatic reaction. The pH dependence of such steps would not be expected to be affected by titrations of single groups in the same way as the pH dependences of the catalytic steps of other GSTs studied (*32*−*38*).

Does rGST T2-2 Function According to a Hysteretic Mechanism? The presence of a conformational transition slower than k_{cat} suggests that stable enzyme−product complexes can be formed that are not on the reaction pathway (k_9/k_{-9}, Figure 2). The fact that k_9^{app} is determined from measurements of changes in intrinsic tryptophan fluorescence validates the assumption that a dynamic, physical step in the enzyme tertiary structure actually is monitored. However, not only the enzyme−product complex would be expected to form such a conformation at equilibrium but in fact all enzyme−ligand complexes in Figure 6 and also the apo-enzyme. Addition of substrate would then cause a so-called ligand-induced slow transition (LIST), a hysteretic effect (cf. ref *39* and references therein). This implies that the detectable

steps represented by the rate constants k_2, k_{-8}, and k_9 are paths leading from an equilibrium state of rGST T2-2 into the catalytically active conformation of the enzyme. In Figure 2, the enzyme forms E′, E″, and E‴ could be considered as steady-state-catalytically active enzyme forms while E represents the favored conformation at equilibrium. The E form requires a substrate-induced conformational transition (e.g., k_2) to enter the catalytical cycle used under steady-state conditions. In principle, catalysis could be performed by enzymes in the "equilibrium−conformation form" as well, but slower than those in the "active" conformation. The rate constants for entering the (faster) catalytic cycle differ depending on the ligand; e.g., going from enzyme−MSG complex involves the slow step represented by k_9 while the apo-enzyme and enzyme−electrophile complex go through k_2. The possible transition between E·G and E′·G was not possible to detect. Either the rate constant for this step is very large or the GSH-liganded conformer is the active species.

If a LIST mechanism applies to rGST T2-2, the reaction scheme in Figure 2 could actually be reduced to that in Figure 6 under steady-state conditions. Flux through the pathway with initial binding of GSH would then be as likely to occur as flux through the other pathway since k_1 and k_3 should both be diffusion controlled.

The presence of a hysteretic mechanism like this would also explain other effects on the kinetics of the enzyme observed. The saturation curves obtained with rGST T2-2 actually fit better to a second degree rate equation than to a first-order Michaelis−Menten or rational function. Non-Michaelian behavior of other GSTs has also been observed (*40*, *41*). An enzyme memory effect has been proposed as an explanation (*42*), but this has later not been taken into account for the sake of simplicity. The LIST mechanism would rationalize the non-Michaelian behavior as a result of substrate addition steps to distinct enzyme forms (*39*), and it would also explain the result from the product inhibition experiment with MSG which was found to be of higher order. MSG release and other steps in the slower catalytic cycle are not shown in Figures 2 and 6. Hill plots derived from kinetic experiments with varying GSH concentrations were found to give curves with slopes of <1, indicating negative cooperativity (results not shown) which is also comprised in the LIST mechanism (*39*). Further, low concentration of the weak inhibitor *S*-propylglutathione added to the assay was found to activate rather than inhibit rGST T2-2. Under steady-state conditions, a low concentration of the inhibitor could assist in keeping the enzyme in the "active" conformation.

Hence, we propose that rGST T2-2 functions according to a hysteretic mechanism. This hypothesis is not irrefutable, but the fact remains that the model accounts for the pre-steady-state and steady-state data presented, and a slow conformational transition was indeed monitored (k_9^{app}, k_{-9}^{app}).

Possible Implications for the Evolution of GSTs. Theta class GSTs are believed to be older from an evolutionary point of view than the alpha, mu, and pi class GSTs (*15*). The GSH-binding domain of the GSTs appears to have a common origin with those from thioredoxin and selenium-dependent glutathione peroxidase (ref *43* and references therein). Through gene fusions and genetic combination, the glutathione-binding motif may have been combined with another protein structure capable of binding hydrophobic molecules, resulting in a protein with affinity for glutathione conjugates (*42*). The strong product inhibition of rGST T2-2, exemplified by the tight binding of MSG supports this hypothesis, if it is assumed that rGST T2-2 represent an ancestral GST structure. Although GSH binds to rat GST T2-2 through several hydrogen bonds (cf. *11*), it is clear from the estimated K_D values for GSH, MS, MSG, and NBSG that the affinity for MS, MSG, and NBSG is stronger than for GSH and that this is due to the hydrophobic naphthylmethyl or benzyl groups of the former. Consequently, hydrophobic interactions were probably the major driving force for binding of the GSH conjugates to the proposed ancestor of the GSTs.

From the perspective of catalysis, the efficiency of rGST T2-2 in catalyzing the first part of the reaction, capturing of substrates followed by fast product formation, is apparently in vain. A product release that is almost 2 orders of magnitude slower than the catalytic step sets the time. Nevertheless, the pH dependence of the pre-steady-state burst of product formation suggests that the catalytic devise of lowering the pK_a of the sulfhydryl group of GSH, making it more nucleophilic, is used by theta as well as by alpha, mu, and pi class GSTs. Thus, this seems to be an old solution to a catalytic problem and perhaps the feature that turned an original GSH−conjugate binding protein into the first GST. The proposed hysteretic mechanism may be a relic from an ancestral protein that displayed catalytically unfavorable tight-binding characteristics. Alpha, mu, and pi class GSTs obviously have evolved toward faster product release, thereby optimizing the GST catalytic properties of what may originally have been a binding protein with a limited catalytic activity.

ACKNOWLEDGMENT

We wish to thank the following colleagues in our department: Dr Leif Grehn for performing NMR analysis on the synthesized MSG, Dr. Gun Stenberg for reviewing the manuscript, and Lars O. Hansson, Per-Olov Markgren, and Dr. Mikael Widersten for valuable discussions.

REFERENCES

1. Mannervik, B., Ålin, P., Guthenberg, C., Jensson, H., Tahir, M. K., Warholm, M., and Jörnvall, H. (1985) *Proc. Natl. Acad. Sci. U.S.A. 82*, 7202−7206.
2. Meyer, D. J., Coles, B., Pemble, S. E., Gilmore, K. S., Fraser, G. M., and Ketterer, B. (1991) *Biochem. J. 274*, 409−414.
3. Meyer, D. J., and Thomas, M. (1995) *Biochem. J. 311*, 739−742.
4. Pemble, S. E., Wardle, A. F., and Taylor, J. B. (1996) *Biochem. J. 319*, 749−754.
5. Board, P. G., Baker, R. T., Chelvanayagam. G., and Jermiin, L. S. (1997) *Biochem. J. 328*, 929−935.
6. Hayes, J. D., and Pulford, D. J. (1995) *Crit. Rev. Biochem. Mol. Biol. 30*, 445−600.
7. Mannervik, B., and Widersten, M. (1995) in *Advances in Drug Metabolism in Man* (Pacifici, G. M., and Fracchia, G. N., Eds.) pp 407−459, European Commission, Luxembourg.
8. Hiratsuka, A., Sebata, N., Kawashima, K., Okuda, H., Ogura, K., Watabe, T., Satoh, K., Hatayama, I., Tsuchida S., Ishikawa, T., and Sato, K. (1990) *J. Biol. Chem. 265*, 11973−11981.
9. Board, P. G., Coggan, M., Wilce, M. C. J., and Parker, M. W. (1995) *Biochem. J. 311*, 247−250.

10. Tan, K.-L., Chelvanayagam, G., Parker, M. W., and Board, P. G. (1996) *Biochem. J. 319*, 315−321.
11. Rossjohn, J., McKinstry, W. J., Oakley, A. J., Verger, D., Flanagan, J., Chelvanayagam, G., Tan, K.-L., Board, P. G., and Parker, M. W. (1998) *Structure 6*, 309−322.
12. Wilce, M. C. J., Board, P. G., Feil, S. C., and Parker, M. W. (1995) *EMBO J. 14*, 2133−2143.
13. Reinemer, P., Prade, L., Hof, P., Neuefeind, T., Huber, R., Zettl, R., Palme, K., Schell, J., Koelln, I., Bartunik, H. D., and Bieseler, B. (1996) *J. Mol. Biol. 255*, 289−309.
14. Armstrong, R. N. (1997) *Chem. Res. Toxicol. 10*, 2−18.
15. Pemble, S. E., and Taylor, J. B. (1992) *Biochem. J. 287*, 957−963.
16. Gillham, B. (1973) *Biochem. J. 135*, 797−804.
17. Gillham, B. (1971) *Biochem. J. 121*, 667−672.
18. Ogura, K., Nishiyama, T., Okada, T., Kajita, J., Narihata, H., Watabe, T., Hiratsuka, A., and Watabe, T. (1991) *Biochem. Biophys. Res. Commun. 181*, 1294−1300.
19. Mannervik, B., Awasthi, Y. C., Board, P. G., Hayes, J. D., Di Ilio, C., Ketterer, B., Listowsky, I., Morgenstern, R., Muramatsu, M., Pearson, W. R., Pickett, C. B., Sato, K., Widersten, M., and Wolf, C. R. (1992) *Biochem. J. 282*, 305−306.
20. Jemth, P., Stenberg, G., Chaga, G., and Mannervik, B. (1996) *Biochem. J. 316*, 131−136.
21. Hyde, C. W., and Young, L. (1968) *Biochem. J. 107*, 519−522.
22. Clapp, J. J., and Young, L. (1970) *Biochem. J. 118*, 765−771.
23. Habig, W. H., Pabst, M. J., and Jakoby, W. B. (1974) *J. Biol. Chem. 249*, 7130−7139.
24. Bardsley, W. G., Bukhari, N. A. J., Ferguson, M. W. J., Cachaza, J. A., and Burguillo, F. J. (1995) *Comput. Chem. 19*, 75−84.
25. Segel, I. H. (1975) *Enzyme Kinetics. Behavior and Analysis of Rapid Equilibrium and Steady-state Enzyme Systems*, pp 273−345, John Wiley & Sons, New York.
26. Mannervik, B. (1982) *Methods Enzymol. 87*, 370−390.
27. Brouwer, A. C., and Kirsch J. F. (1982) *Biochemistry 21*, 1302−1307.
28. Graminski, G. F., Kubo, Y., and Armstrong, R. N. (1989) *Biochemistry 28*, 3562−3568.
29. Fersht, A. (1998) *Structure and Mechanism in Protein Science: A Guide to Enzyme Catalysis and Protein Folding*, pp 132−190, W. H. Freeman and Co., New York.
30. Beece, D., Eisenstein, L., Frauenfelder, H., Good, D., Marden, M. C., Reinisch, L., Reynolds, A. H., Sorensen, L. B., and Yue, K. T. (1980) *Biochemistry 19*, 5147−5157.
31. Bazelyansky, M., Robey, E., and Kirsch, J. F. (1986) *Biochemistry 25*, 125−130.
32. Caccuri, A. M., Lo Bello, M., Nuccetelli, M., Nicotra, M., Rossi, P., Antonini, G., Federici, G., and Ricci, G. (1998) *Biochemistry 37*, 3028−3034.
33. Jemth, P., and Mannervik, B. (1997) *Arch. Biochem. Biophys. 348*, 247−254.
34. Chen, W.-J., Graminski, G. F., and Armstrong, R. N. (1988) *Biochemistry 27*, 647−654.
35. Wang, R. W., Newton, D. J., Huskey, S.-E. W., McKeever, B. M., Pickett, C. B., and Lu, A. Y. H. (1992) *J. Biol. Chem. 267*, 19866−19871.
36. Kong, K.-H., Inoue, H., and Takahashi, K. (1992) *J. Biochem. 112*, 725−728.
37. Ji, X., von Rosenvinge, E. C., Johnson, W. W., Tomarev, S. I., Piatigorsky, J., Armstrong, R. N., and Gilliland, G. L. (1995) *Biochemistry 34*, 5317−5328.
38. Widersten, M., Björnestedt, R., and Mannervik, B. (1996) *Biochemistry 35*, 7731−7742.
39. Neet, K. E. (1996) in *Contemporary Enzyme Kinetics and Mechanism* (Purich, D. L., Ed.) 2nd ed., pp 154−159, Academic Press, San Diego.
40. Pabst, M. J., Habig, W. H., and Jakoby, W. B. (1974) *J. Biol. Chem. 249*, 7140−7150.
41. Askelöf, P., Guthenberg, C., Jakobson, I., and Mannervik, B. (1975) *Biochem. J. 147*, 513−522.
42. Mannervik, B. (1985) *Adv. Enzymol. Relat. Areas Mol. Biol. 57*, 357−417.
43. Mannervik, B., Carlberg, I., and Larson, K. (1989) in *Coenzymes and Cofactors* (Dolphin, D., Poulson, R., and Avramovic, O., Eds.) Vol. 3A, pp 475−516, Wiley, New York.

BI983065B